ACS APPLIED MATERIALS & INTERFACES

Research Article

www.acsami.org

Synthesis and Electrophosphorescence of Iridium Complexes Containing Benzothiazole-Based Ligands

Di Liu,* Huicai Ren, Lijun Deng, and Ting Zhang

State Key Laboratory of Fine Chemicals, School of Chemistry, Dalian University of Technology, 2 Linggong Road, Dalian 116024, China

Supporting Information

ABSTRACT: Four heteroleptic bis-cyclometalated iridium(III) complexes containing 2-aryl-benzothiazole ligands, in which the aryl is dibenzofuran-2-yl [$Ir(O\text{-}bt)_2(acac)$], dibenzothiophene-2-yl [$Ir(S\text{-}bt)_2(acac)$], dibenzothiophene-S,S-dioxide-2-yl [$Ir(SO_2\text{-}bt)_2(acac)$] and 4-(diphenylphosphoryl)phenyl [$Ir(PO\text{-}bt)_2(acac)$], have been synthesized and characterized for use in organic light-emitting diodes (OLEDs). These complexes emit bright yellow (551 nm) to orange-red (598 nm) phosphorescence at room temperature, the peak wavelengths of which can be finely tuned depending upon the electronic properties of the aryl group in the 2-position of benzothiazole. The strong electron-withdrawing aryls such as dibenzothiophene-S,S-dioxide2-yl and 4-(diphenylphosphoryl)phenyl caused bathochromatic shift of the iridium complex phosphorescence. These iridium complexes were used as doped emitters to fabricate yellow to orange-red OLEDs and good performance was obtained. In particular, a maximum luminance efficiency of 58.4 cd A^{-1} (corresponding to 30.6 lm W^{-1} and 19%) with CIE coordinates of (0.45, 0.52) was achieved for $Ir(O\text{-}bt)_2(acac)$-based yellow device. Furthermore, the yellow emitting $Ir(S\text{-}bt)_2(acac)$ was used to fabricate two-element white OLED that exhibited a high efficiency of 32.4 cd A^{-1} with CIE coordinates of (0.28, 0.44).

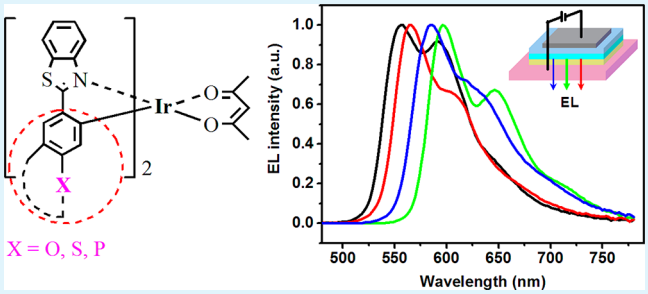

KEYWORDS: *OLED, electrophosphorescence, iridium complex, benzothiazole, bathochromatic shift, yellow*

INTRODUCTION

Phosphor complex emitters prepared with a third-row transition-metal element such as Ir, Os, and Pt are crucial for the fabrication of highly efficient organic light-emitting diodes (OLEDs).[1−4] These complexes can harvest both singlet and triplet excitons to realize a theoretical internal quantum efficiency of 100% due to the strong spin−orbit coupling of the heavy-metal ion that leads to efficient intersystem crossing of the singlet excited states to the triplet manifold.[5] To meet the target of full-color flat-panel displays and low-cost solid-state lighting, researchers have directed their attention to the color-tuning of these materials. Among the above phosphor emitters, cyclometalated iridium(III) complexes, which have relatively short excited-state lifetime, high phosphorescence efficiency and flexible color tunability, are regarded as the most promising phosphors in OLEDs.[6,7] Generally, the emission colors of the iridium complexes are strongly dependent on the cyclometalating ligands, its substituent groups and/or ancillary ligands.[8,9]

2-Phenylbenzothiazole is one typical ligand framework to construct iridium complexes giving efficient yellow emission. There have been many reports on the color-tuning of iridium complexes based on 2-phenylbenzothiazole ligands. However, most of the structure modification were achieved by introducing simple electron-donating/withdrawing (OMe, Me, CF_3, F, CN, etc.) groups or a more extended chromophore either to the phenyl ring or to the benzothiazole moiety.[10−12] Furthermore, the phosphorescence of the current iridium complexes based on this 2-phenylbenzothiazole ligand framework is mainly localized within a narrow color range around yellow[13] with few exceptions. This definitely limits their applications in full-color OLEDs products. As far as we know, the study of the iridium complexes containing 2-aryl-benzithiazole ligand frameworks, in which the aryl is aromatic skeletons other than phenyl, has not been reported so far.

Our interest is to develop novel ligand frameworks by replacing the free phenyl ring in 2-phenylbenzothiazole with other aryl groups, such as dibenzofuran, dibenzothiophene, dibenzothiophene-S,S-dioxide, and 4-(diphenylphosphoryl)-phenyl. In this paper, we report the synthesis and properties of these novel ligands (Scheme 1) and their heteroleptic bis-cyclometalated iridium complexes $Ir(O\text{-}bt)_2(acac)$, $Ir(S\text{-}bt)_2(acac)$, $Ir(SO_2\text{-}bt)_2(acac)$, and $Ir(PO\text{-}bt)_2(acac)$ (Scheme 2) with the widely used acetylacetone (acac) as ancillary ligand.[8] The former three ligands, O-bt, S-bt, and SO_2-bt, have the same molecular skeletons. However, the atom or group (O, S, SO_2) at the 5-site of the aryl ring has different electronic properties, which probably have a different influence on the

Received: February 22, 2013
Accepted: May 20, 2013
Published: May 20, 2013

   dx.doi.org/10.1021/am400672y | ACS Appl. Mater. Interfaces 2013, 5, 4937−4944

Scheme 1. Synthesis of the Ligands

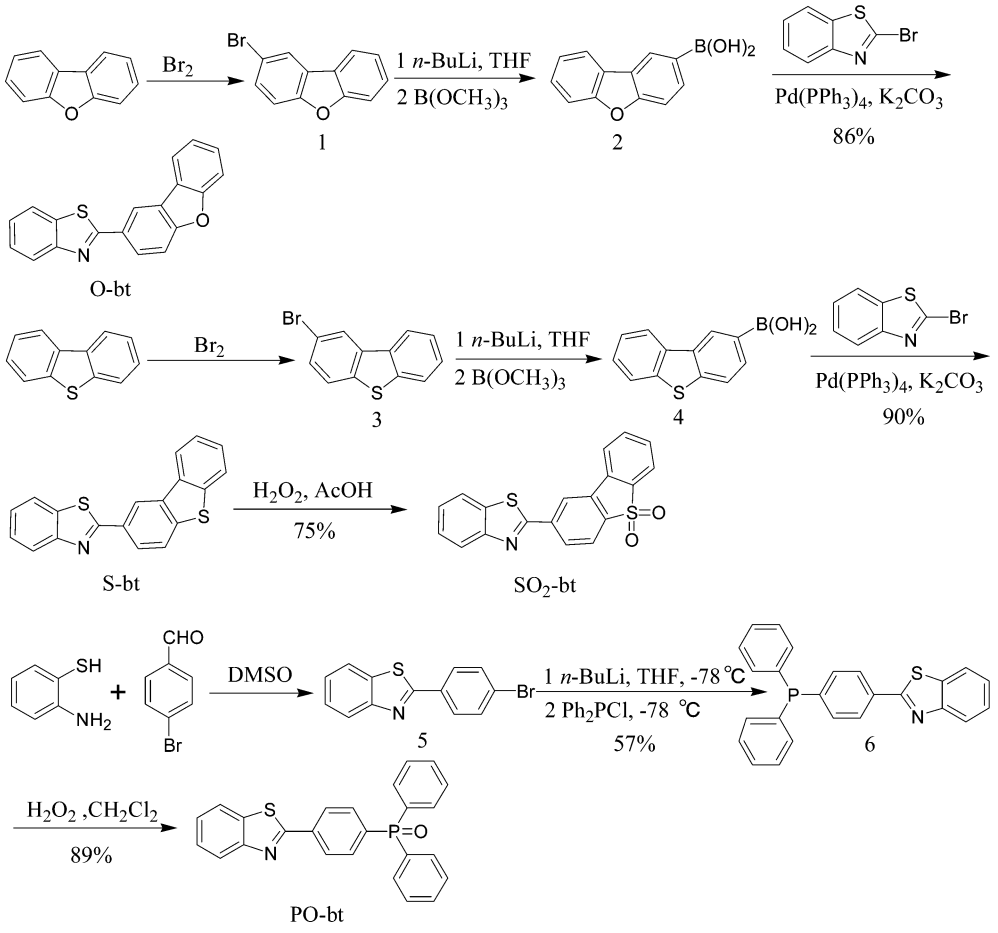

luminescent behavior of the iridium complexes. For ligand PO-bt, it can be regarded as the 2-phenylbenzothiazole derivative with diphenylphosphoryl substituent at the para-site of the phenyl ring. In comparison with the former three ligands, the diphenylphosphoryl substituent is at the similar position. However, it is different in that the two phenyl rings on the phosphoryl group are rotatable and the ligand is not as rigid as the former three ones. All these structural features are expected to lead to interesting properties for the iridium complexes. The photophysical and electrochemical properties and the electroluminescent performance in OLEDs of these complexes were investigated. All these complexes emit strong phosphorescence at room temperature with emitting color spanning from yellow to orange-red. Efficient phosphorescent OLEDs were obtained using these complexes as doped emitters. Notably, a maximum luminance of 65633 cd m^{-2} and a peak luminance efficiency of 58.4 cd A^{-1} were realized for $Ir(O\text{-}bt)_2(acac)$-based yellow-emitting device. In addition, because of the increasing interest in developing yellow/orange phosphors for two-color WOLEDs in recent years,[12,14,15] the yellow emitting $Ir(S\text{-}bt)_2(acac)$ was also used to fabricate two-element white OLED, achieving good performance with a high efficiency of 32.4 cd A^{-1}.

EXPERIMENTAL SECTION

Materials, Instruments, and Methods. All the reagents are of analytical grade and used as received from commercial sources without further purification. PEDOT:PSS was purchased from Bayer AG. The solvents used in the reactions were purchased from Aldrich and were treated to be anhydrous using the standard methods.

^1H NMR and ^{13}C NMR spectra were recorded on a 400 or 100 MHz Varian Unity Inova spectrophotometer. Mass spectra were taken on MALDI micro MX and HP1100LC/MSD MS spectrometers. The photoluminescence and UV−vis absorption spectra measurements were performed on a Perkin-Elmer LS55 spectrometer and a Perkin-Elmer Lambda 35 spectraphotometer, respectively. Phosphorescence lifetimes were measured on an Edinburgh FLS920 Spectrometer in degassed dichloromethane solutions.

Cyclic voltammetry (CV) measurements were performed using a conventional three-electrode cell with a glassy carbon working electrode, a platinum wire counter electrode, and a saturated calomel electrode reference electrode on a computer-controlled BAS 100W electrochemical analyzer at room temperature. The complexes were dissolved in dichloromethane solution containing Bu_4NPF_6 (0.1 M) as a supporting electrolyte. The redox potentials were obtained at the scan rate of 100 mV/s, and with ferrocene/ferrocenium (Fc/Fc^+) as an internal standard of the redox system.

OLED Fabrication and Measurements. The patterned ITO substrates were cleaned by successive ultrasonications in detergent, deionized water, ethanol, and chloroform, followed by treatment with UV-ozone. PEDOT:PSS (Bayer AG) was spin-coated on pretreated ITO substrate from aqueous dispersion and baked at 120 °C for 1 h. All the organic layers except complex $Ir(PO\text{-}bt)_2(acac)$ were deposited by vacuum evaporation in a vacuum chamber with a base pressure less than 1×10^{-6} Torr. The device containing complex $Ir(PO\text{-}bt)_2(acac)$ was prepared with an emitting layer made by the spin-coating method because of the poor sublimation ability of this complex. The emitting area of each pixel was determined by overlapping of anode and cathode as 9 mm^2. The EL spectra, CIE coordinates, and current−voltage−luminance characteristics were measured with computer-controlled Spectrascan PR 705 photometer and a source-measure-unit Keithley 236 under ambient conditions. The forward viewing external

Scheme 2. Synthesis of the Novel Iridium Complexes

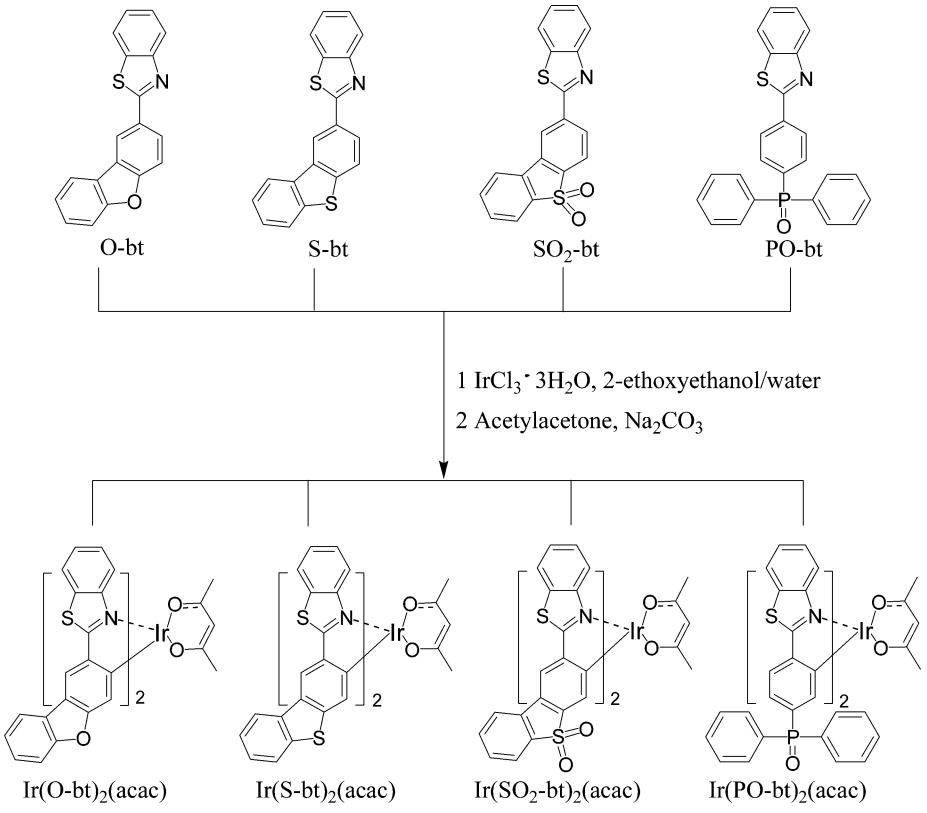

quantum efficiency (η_{ext}) was calculated using the luminance efficiency, EL spectra, and human photopic sensitivity.

The synthesis of ligands and important intermediates is provided in the Supporting Information.

General Procedure for Synthesis of Iridium Complexes. A mixture of the ligand (2.5 equiv.) and iridium trichloride in 2-ethoxyethanol:water (3:1 v/v) was stirred at 100 °C under nitrogen for 12 h. The mixture was cooled to room temperature and the precipitate was collected and washed with ethanol and then dried in vacuum to give the corresponding cyclometalated Ir(III)-μ-chloro-bridged dimer. Then the dimer complex, acetylacetone (5 equiv.) and Na_2CO_3 (10 equiv.) were mixed in degassed 2-ethoxyethanol (15 mL) and the mixture was refluxed at 120 °C under nitrogen for 24 h. Upon cooling, the precipitation was filtered off and the residue was purified on a silica gel column to afford the desired iridium complex.

Ir(O-bt)$_2$(acac). Orange powder, yield 24%. ^{1}H NMR (400 MHz, $CDCl_3$) δ (ppm): 8.24 (s, 2H, ArH), 8.10−8.14 (m, 2H, ArH), 7.92−7.94 (m, 2H, ArH), 7.80−7.82 (d, J = 8.0 Hz, 2H, ArH), 7.43−7.46 (m, 4H, ArH), 7.22−7.27 (m, 4H, ArH), 7.17−7.21 (m, 2H, ArH), 6.56 (s, 2H, ArH), 5.22 (s, 1H, =CH−), 1.85 (s, 6H, $-CH_3$). ^{13}C NMR (100 MHz, $CDCl_3$) δ (ppm):185.9, 180.1, 157.9, 155.3, 150.9, 148.3, 137.1, 131.3, 127.5, 126.1, 125.3, 124.7, 122.7, 122.4, 120.1, 119.6, 119.2, 118.4, 116.9, 111.25, 101.9, 53.4, 28.4. MALDI-TOF-MS (m/z): 892.3086 ([M]$^+$). Elemental anal. Calcd for $C_{43}H_{27}IrN_2O_4S_2$: C, 57.90; H, 3.05; N, 3.14; S, 7.19. Found: C, 57.53; H, 3.11; N, 3.02; S, 7.01.

Ir(S-bt)$_2$(acac). Orange powder, yield 29%. ^{1}H NMR (400 MHz, $CDCl_3$) δ (ppm): 8.43 (s, 2H, ArH), 8.08−8.11 (m, 4H, ArH), 7.98−8.00 (d, J = 8.0 Hz, 2H, ArH), 7.61−7.63 (d, J = 8.0 Hz, 2H, ArH), 7.46−7.50 (m, 4H, ArH), 7.30−7.33 (m, 4H, ArH), 6.85 (s, 2H, ArH), 5.30 (s, 1H, =CH−), 1.77 (s, 6H, $-CH_3$). ^{13}C NMR (100 MHz, $CDCl_3$) δ (ppm): 185.9, 180.1, 150.9, 143.1, 139.0, 138.0, 135.9, 131.3, 130.3, 128.0, 127.6, 125.7, 125.4, 124.3, 122.6, 122.4, 120.3, 120.2, 118.7, 101.7, 53.4, 28.4.MALDI-TOF-MS (m/z): 924.1036 ([M]$^+$). Elemental anal. Calcd for $C_{43}H_{27}IrN_2O_2S_4$: C, 55.88; H, 2.94; N, 3.03; S, 13.88. Found: C, 55.34, H, 2.82; N, 2.99; S, 13.63.

Ir(SO$_2$-bt)$_2$(acac). Orange-red powder, yield 12%. ^{1}H NMR (400 MHz, DMSO) δ (ppm): 8.74 (s, 2H, ArH), 8.45−8.47 (t, 2H, ArH), 8.29−8.31 (d, J = 8.0 Hz, 2H, ArH), 7.97−7.99 (m, 2H, ArH), 7.75−7.82 (m, 4H, ArH), 7.69−7.71 (m, 4H, ArH), 7.52−7.56 (t, 2H, ArH), 6.59 (s, 2H, ArH), 5.25 (s, 1H, =CH−), 1.77 (s, 6H, $-CH_3$). ^{13}C NMR (100 MHz, DMSO) δ (ppm): 186.7, 179.1, 152.2, 149.9, 147.7, 137.5, 136.0, 134.9, 132.4, 131.9, 130.4, 129.0, 127.3, 126.2, 125.8, 124.9, 122.7, 122.2, 120.5, 119.7, 102.2, 55.4, 28.3. MALDI-TOF-MS (m/z): 1011.0179 ([M+Na]$^+$). Elemental anal. Calcd for $C_{43}H_{27}IrN_2O_6S_4$: C, 52.26; H, 2.75; N, 2.83; S, 12.98. Found: C, 52.03; H, 2.86; N, 2.57; S, 12.74.

Ir(PO-bt)$_2$(acac). Orange-red powder, yield 31%. ^{1}H NMR (400 MHz, $CDCl_3$) δ (ppm): 7.89−7.91 (d, J = 8.0 Hz, 2H, ArH), 7.81−7.83 (d, J = 8.0 Hz, 2H, ArH), 7.65−7.68 (m, 2H, ArH), 7.42−7.49 (m, 4H, ArH), 7.26−7.36 (m, 12H, ArH),7.16−7.19 (t, 2H, ArH), 7.08−7.13 (m, 8H, ArH), 6.14−6.17 (d, J = 12 Hz, 2H, ArH), 5.29 (s, 1H, =CH−), 1.74 (s, 6H, $-CH_3$). ^{13}C NMR (100 MHz, $CDCl_3$) δ (ppm): 150.3, 147.2, 144.9, 138.2, 133.5, 132.8, 132.6, 132.5, 131.8−131.2, 128.1−127.7, 127.5, 125.6, 125.4, 125.3, 124.8, 122.4, 120.2, 101.7, 60.4, 28.2. MALDI-TOF-MS (m/z): 1135.1221 ([M+Na]$^+$). Elemental anal. Calcd for $C_{55}H_{41}IrN_2O_4S_2P_2$: C, 59.39; H, 3.72; N, 2.52; S, 5.77. Found: C, 59.02; H, 3.42; N, 2.47; S, 5.33.

RESULTS AND DISCUSSION

Synthesis. The cyclometalating ligands, O-bt, S-bt, SO_2-bt, and PO-bt, were synthesized according to the procedure described in Scheme 1. The commercially available dibenzofuran and dibenzothiophene were first brominated to afford 2-bromodibenzofuran and 2-bromodibenzothiophene, respectively. These bromides were then treated with *n*-BuLi followed by reaction with trimethyl borate and then hydrolyzed to afford dibenzofuran- and dibenzothiophene-2-ylboronic acids. Then Suzuki-coupling of the corresponding boronic acid with 2-bromobenzothiazole yielded the target ligand O-bt or S-bt. Further oxidation of ligand S-bt with an excess of 30% H_2O_2 in

Table 1. Photophysical Data of the Ir Complexes

complexes	$\lambda_{abs.}$ (log ε) (nm)[a]	λ_{em} (nm)[a]	Φ_{PL}[c]	τ_p (μs)[d]	HOMO (eV)	LUMO[e] (eV)	E_g[f] (eV)
Ir(O-bt)$_2$(acac)	339(4.58), 395 (3.78), 458(3.48)	551 (587 sh)[b]	0.10	2.28	−5.18	−2.88	2.30
Ir(S-bt)$_2$(acac)	331 (4.66), 403 (3.84), 472(3.48)	562 (602 sh)	0.11	2.34	−5.18	−2.90	2.28
Ir(SO$_2$-bt)$_2$(acac)	326 (5.2), 359 (4.96),433(4.15),518 (3.92)	598 (646 sh)	0.29	1.53	−5.47	−3.30	2.17
Ir(PO-bt)$_2$(acac)	323(4.66),374 (4.11), 459 (3.95), 507 (3.86)	583 (628 sh)	0.23	1.66	−5.38	−3.17	2.21

[a]Measured in CH_2Cl_2 at a concentration of 1.0×10^{-5} mol L^{-1}. [b]sh = shoulder. [c]In degassed toluene relative to *fac*-Ir(ppy)$_3$ (Φ_{PL} = 0.40). [d]In degassed CH_2Cl_2 at room temperature. [e]LUMO = HOMO + E_g. [f]Estimated from the absorption edge (λ_{edge}) of solid film by equation of E_g = 1240/λ_{edge}.

acetic acid generated the ligand SO$_2$-bt as a white solid. As for the preparation of ligand PO-bt, a different procedure was utilized. First the intermediate 5 was obtained by reaction of 2-aminothiophenol with 4-bromobenzaldehyde in DMSO at 195 °C. A lithium-halogen exchange reaction between compound 5 and *n*-BuLi followed by reaction with chlorodiphenylphosphine gave compound 6, further oxidation of which with 30% H_2O_2 in dichloromethane generated the target ligand PO-bt.

The desired iridium(III) complexes, Ir(O-bt)$_2$(acac), Ir(S-bt)$_2$(acac), Ir(SO$_2$-bt)$_2$(acac) and Ir(PO-bt)$_2$(acac), were then prepared following the typical two-step procedure that involves the preliminary synthesis of the corresponding dichloro-bridged dimer complexes and subsequent reaction of the intermediates with acetylacetone in presence of Na_2CO_3.[8] The synthetic procedure of these novel iridium complexes are outlined in Scheme 2. These products are well-dissolved in most common organic solvents and are able to be purified by silica-gel column chromatography. The chemical structures are unambiguously characterized by ^{1}H and ^{13}C NMR and MALDI-TOF mass spectrometry.

Photophysical Properties. The UV−vis and photoluminescence (PL) data of the iridium complexes are summarized in Table 1. The absorption spectra of all the ligands are also measured for comparison. As shown by the electronic absorption spectra in Figure S1 in the Supporting Information, all the ligands have an intense absorption below 360 nm because of the spin-allowed $\pi-\pi^*$ transition. The absorption spectra and fluorescence spectra for these iridium complexes are shown in Figures 1 and 2, respectively. In common with most iridium complexes, there are two major absorption bands for each of the present complexes. The intense bands in the short wavelength region below 400 nm appear to be ligand-based transitions which closely resemble the spectra of the free ligands.[16] The weaker absorptions arising in the range of 400−550 nm are likely due to metal-to-ligand

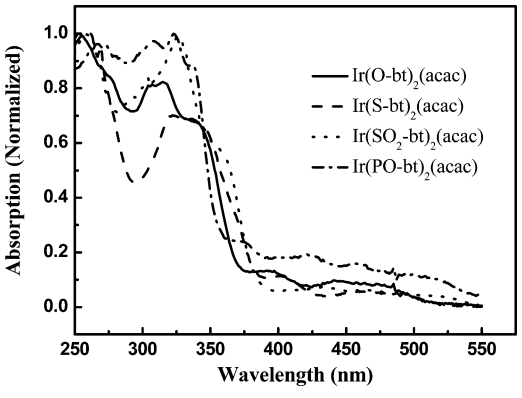

Figure 1. Absorption spectra of the iridium complexes in CH_2Cl_2 solutions.

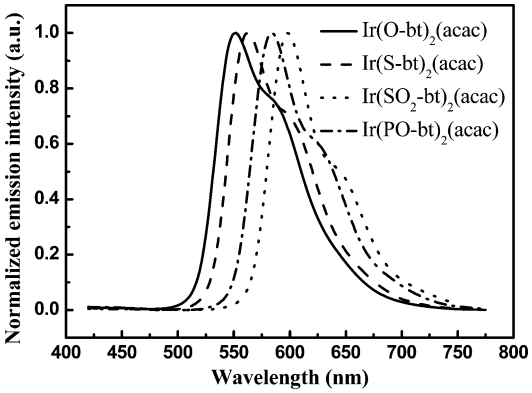

Figure 2. PL spectra of iridium complexes in CH_2Cl_2 solutions at room temperature (λ_{exc} = 400 nm).

charge-transfer transitions (^{1}MLCT and ^{3}MLCT) and the spin−orbit coupling enhanced $^3\pi-\pi^*$ states.[17,18] Upon photoexcitation at 400 nm at room temperature, these complexes emit bright yellow to orange-red luminescence in dilute dichloromethane solutions. For example, Ir(O-bt)$_2$(acac) exhibits yellow phosphorescence with peak at 551 nm and a shoulder at 587 nm, whereas Ir(SO$_2$-bt)$_2$(acac) is orange-red emissive with peak at 598 nm and a shoulder at 646 nm. Obviously, with varying the aryl group in the 2-arylbenzothiazole ligands, a regular red-shift of the phosphorescence peak wavelength was observed in the following order: Ir(O-bt)$_2$(acac) < Ir(S-bt)$_2$(acac) < Ir(PO-bt)$_2$(acac) < Ir(SO$_2$-bt)$_2$(acac), as indicated by the photoluminescence (PL) spectra in Figure 2. A redshift of 11 nm was observed for the phosphorescence of Ir(S-bt)$_2$(acac) (562 nm) relative to Ir(O-bt)$_2$(acac) (551 nm) despite having the same molecular skeletons and similar electronic properties of O and S atoms. This is probably because S is more polarizable than O, resulting in an enhanced conjugative effect in ligand S-bt[17,18] and thus the lower-energy excited states for both the ligand S-bt and the complex Ir(S-bt)$_2$(acac). In comparison with Ir(O-bt)$_2$(acac) and Ir(S-bt)$_2$(acac), the strong electron-withdrawing sulphonyl and diphenylphosphoryl-based complexes Ir(SO$_2$-bt)$_2$(acac) and Ir(PO-bt)$_2$(acac) exhibit phosphorescence at much longer wavelengths. This is consistent with the relative longer-wavelength absorption edges of these two complexes as shown in Figure 1 and thus the lower energy band gaps for these two molecules.

The phosphorescent quantum yields (Φ_{PL}) of these complexes were measured at 298 K in degassed toluene solutions using Ir(ppy)$_3$ (Φ_{PL} = 0.40 in toluene)[19] as standard and were calculated as 0.10−0.29. The room-temperature emission lifetimes of these complexes in dichloromethane solutions were determined in the range of 1.53−2.34 μs, which

are consistent with the emission from the triplet excited states.[20]

Electrochemistry and Theoretical Calculations. The redox behavior of these complexes was investigated by cyclic voltammetry measurements in anhydrous dichloromethane solutions under argon atmosphere, using Bu_4NPF_6 as the electrolyte. The electrochemical and electronic data are summarized in Table 1 and cyclic voltammograms are illustrated in Figure 3. During the anodic scan, each of these

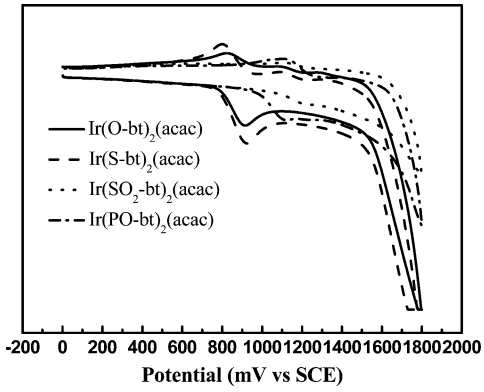

Figure 3. Cyclic voltammograms of Ir(III) complexes.

iridium complexes undergoes a reversible one-electron oxidation, which is assigned to the metal-centered Ir(III)/Ir(IV) oxidation couple. However, no reduction process was detected in dichloromethane under present conditions. The onset potentials of the first oxidation wave (E^{ox}_{onset}) are both at 0.78 V vs saturated calomel electrode (SCE) for complex Ir(O-bt)$_2$(acac) and Ir(S-bt)$_2$(acac). The oxidation potentials for Ir(PO-bt)$_2$(acac) and Ir(SO$_2$-bt)$_2$(acac) shifted to more positive values of 0.98 and 1.07 V as compared with Ir(O-bt)$_2$(acac) and Ir(S-bt)$_2$(acac), indicating that the oxidation becomes harder with the presence of the phosphoryl and sulphonyl groups. This is reasonable if the strong electron-withdrawing nature of these two groups is taken into account, which definitely makes it more difficult for the corresponding iridium complex to lose an electron and get oxidized. On the basis of the E^{ox}_{onset} data, the HOMO levels were determined using the empirical formulate of $E_{HOMO} = -e(E^{ox}_{onset} + 4.4)$[21,22] as −5.18 to −5.38 eV. Apparently, these HOMO levels are close to the energy levels of most hole injecting and transporting materials, being favorable for electron injection into these iridium phosphors when used as doped emitter in OLEDs. The LUMO energies were determined by equation of $E_{LUMO} = E_{HOMO} + E_g$, where E_g is the optical energy gap and is obtained by absorption edge technique (Table 1).[21,22] In this way, the LUMO levels of these iridium complexes are determined in the range of −2.88 to −3.30 eV. Evidently, the incorporation of the electron-withdrawing diphenylphosphoryl and sulphonyl groups in complexes Ir(PO-bt)$_2$(acac) and Ir(SO$_2$-bt)$_2$(acac) causes the descending of both HOMO and LUMO levels. However, the larger downward shift of LUMO than HOMO leads to smaller HOMO−LUMO band gaps for Ir(PO-bt)$_2$(acac) and Ir(SO$_2$-bt)$_2$(acac) in comparison with Ir(O-bt)$_2$(acac) and Ir(S-bt)$_2$(acac). These electrochemical data are in good agreement with the optical observation that Ir(PO-bt)$_2$(acac) and Ir(SO$_2$-bt)$_2$(acac) are emissive at much longer wavelengths than Ir(O-bt)$_2$(acac) and Ir(S-bt)$_2$(acac).

For better understanding the structure−property relationships, we performed density functional theory (DFT) calculations for these four iridium complexes using B3LYP hybrid functional theory with Gaussion 03.[23] Figure 4 illustrates the spatial distribution of the HOMO and LUMO orbitals. For all these four complexes, their HOMO are localized on the central iridium atom and the aryl part in the 2-aryl-benzothiazole ligand, with the major contribution from the phenyl ring that is directly linked to the iridium atom, while their LUMO spread from the benzothiazole part to the directly linked phenyl ring. The spatial distribution of the frontier molecular orbitals for these conplexes is similar to the case when the cyclometalating ligand is 2-phenyl-benzothiazole.[24] However, in comparison with Ir(O-bt)$_2$(acac) and Ir(S-bt)$_2$(acac), the LUMO for Ir(PO-bt)$_2$(acac) and Ir(SO$_2$-bt)$_2$(acac) spread more to the aryl direction. This should be because of the strong electron-withdrawing effect of the sulphonyl and phosphoryl groups, consistent with the photophysical and electrochemical observation.

Electrophosphorescent OLEDs. To evaluate the electroluminescent properties of these iridium complexes, OLEDs were fabricated using them as doped emitters. On the basis of the good thermal stability of these complexes, the OLEDs were fabricated by vacuum deposition approach and have the configuration of ITO/PEDOT:PSS (40 nm)/CBP:iridium complex (5 wt %, 30 nm)/TPBI (40 nm)/LiF (1 nm)/Al (150 nm). In these devices, PEDOT:PSS is poly(3,4-

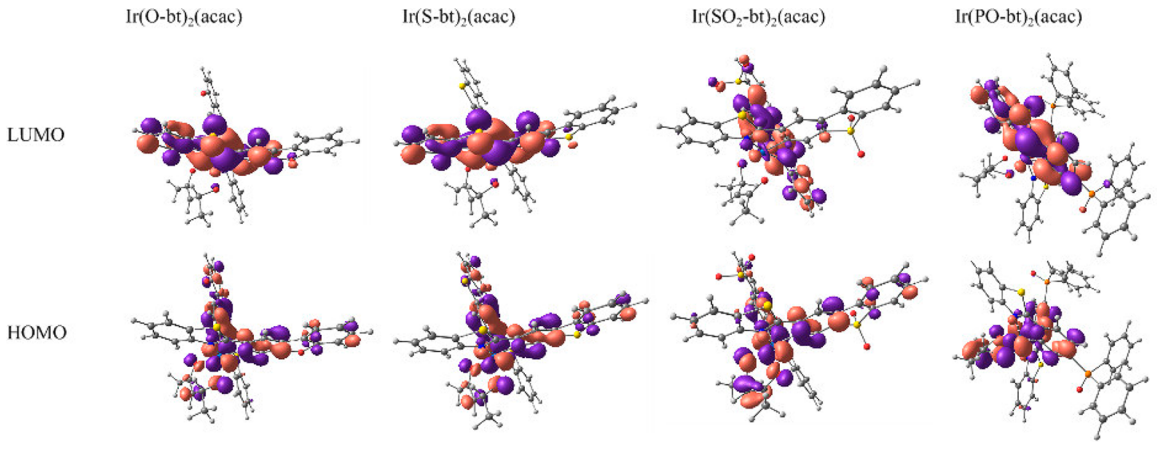

Figure 4. Contour plots of HOMO and LUMO for the iridium complexes.

Table 2. EL Performance of Iridium Complexes

complex	V_{on} (V)	$J_{max}{}^a$ (mA cm^{-2})	$L_{max}{}^a$ (cd m^{-2})	$\eta_L{}^a$ (cd A^{-1})	$\eta_p{}^a$ (lm W^{1-})	$\eta_{ext.}{}^a$ (%)	λ_{EL} (nm)	CIE(x, y) at 8 V
Ir(O-bt)$_2$(acac) (5 wt %)	3.9	337 (12)	65633 (12)	58.4 (6)	30.6 (5)	19 (6)	556 (595 sh)	(0.45, 0.52)
Ir(S-bt)$_2$(acac) (5 wt %)	4	246 (12)	55530 (12)	54.1 (6)	28.3 (6)	19 (6)	566 (606 sh)	(0.51, 0.48)
Ir(SO$_2$-bt)$_2$(acac) (5 wt %)	6	293 (12)	6958 (12)	3.5 (7)	1.6 (7)	2.5 (7)	595 (646 sh)	(0.58, 0.34)
Ir(PO-bt)$_2$(acac) (10 wt %)^b	6	164 (13)	1057 (13)	4.3 (7)	1.9 (7)	2.3 (7)	586 (630 sh)	(0.56, 0.41)
Ir(S-bt)$_2$(acac) + Firpic	4	173 (14)	19760 (14)	32.4 (7)	14.5 (7)		474, 502, 562	(0.28, 0.44)^c

^{a}Maximum values of the devices. Values in parentheses are the voltages at which they were obtained. ^{b}The device was prepared by spin-coating the emitting layer. ^{c}The CIE for WOLED was obtained at 14 V.

ethylenedioxythiophene):poly(styrene sulfonate) and acts as hole-injecting layer, CBP is 4,4′ -*N*,*N*′ -dicarbazolebiphenyl and as host for the iridium phosphors, TPBI is 1,3,5-tris[N-(phenyl)benzimidazole]-benzene and as electron-transporting and hole-blocking material because of its relatively low HOMO level. As an exception, the Ir(PO-bt)$_2$(acac) based device was prepared by partial solution method since Ir(PO-bt)$_2$(acac) is prone to decompose under thermal evaporation. The Ir(PO-bt)$_2$(acac) device has a structure of ITO/PEDOT:PSS (40 nm)/PVK (60 wt %):OXD-7 (30 wt %):Ir(PO-bt)$_2$(acac) (10 wt %, 30 nm)/TPBI (40 nm)/LiF (1 nm)/Al (150 nm), in which PVK [poly(vinylcarbazole)] is used as hole-transporting host, OXD-7 [2,2′-(1,3-Phenylene)bis[5-(4-tert-butylphenyl)-1,3,4-oxadiazole]] was included into the host matrix to facilitate electron transport. The emitting layer was obtained by spin-coating the mixed solution of PVK, OXD-7 and iridium complex in chlorobenzene on top of PEDOT:PSS layer, followed by deposition of TPBI layer and cathode in a vacuum chamber. Table 2 summarizes the important performance data for these devices.

These four OLEDs exhibited bright yellow to orange-red electroluminescence. As depicted in Figure 5, the EL spectra

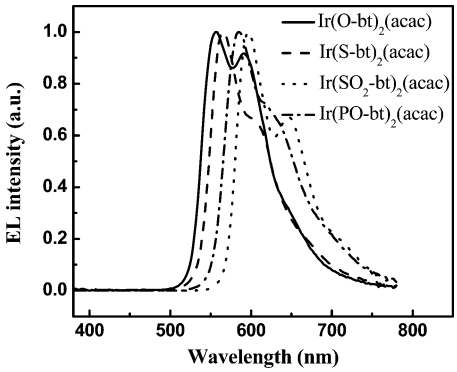

Figure 5. EL spectra of each iridium complex device at 8 V.

profile of each device is identical to the PL spectra of the corresponding iridium complex, suggesting that the EL emission indeed originates from the triplet excited states of the iridium phosphors. The small red-shifts of 3−5 nm were observed for EL spectra in comparison with PL, which is typically assigned to the additional effect of the electrical field on the excited states.[25] The EL spectra are found to be independent of the driving voltages, as shown by the spectra of Ir(S-bt)$_2$(acac) device in Figure S2 in the Supporting Information, indicating the excellent spectral stability. Additionally, no residual emission from CBP or TPBI is observed in these devices even at high voltages, implying the efficient forward energy transfer from the host exciton to the phosphor molecules and effective confinement of the excitons on the iridium phosphors rather than exciton diffusion to adjacent layers.

The current density−voltage−luminance (J−V−L) characteristics and current efficiency−current density curves for complex Ir(O-bt)$_2$(acac)-, Ir(S-bt)$_2$(acac)-, and Ir(SO$_2$-bt)$_2$(acac)-based devices are shown in Figure 6. The Ir(O-bt)$_2$(acac)-doped device exhibited the best performance with a turn-on voltage (to deliver a brightness of 1 cd m^{-2}) of 3.9 V, and a maximum luminance (L_{max}) of 65633 cd m^{-2} at 12 V, a peak luminance efficiency (η_L) of 58.4 cd A^{-1}, corresponding to a peak power efficiency (η_p) of 30.6 lm W^{-1} and a peak external quantum efficiency (η_{ext}) of 19%. It is obvious that a peak luminance efficiency of 58.4 cd A^{-1} for Ir(O-bt)$_2$(acac)-doped device is among the best data for the yellow OLEDs reported so far.[10,26] The performance of Ir(S-bt)$_2$(acac)-based device is also remarkable, with a L_{max} of 55530 cd m^{-2} at 12 V, and a η_L of 54.1 cd A^{-1} at 6 V, and a η_p of 28.3 lm W^{-1} at 6 V. Although the phosphorescence quantum efficiency of Ir(SO$_2$-bt)$_2$(acac)

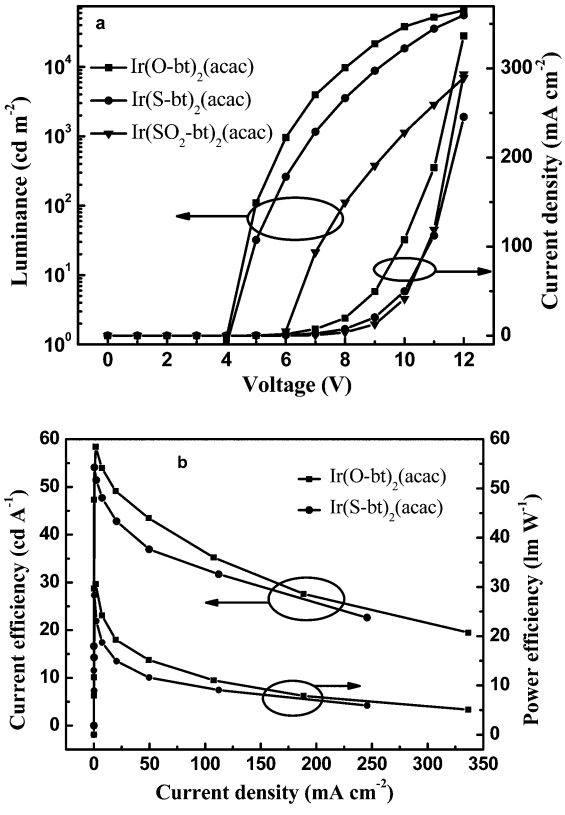

Figure 6. (a) J−V−L characteristics for Ir(O-bt)$_2$(acac)-, Ir(S-bt)$_2$(acac)-, and Ir(SO$_2$-bt)$_2$(acac)-based OLEDs; and (b) the efficiency curves for Ir(O-bt)$_2$(acac)- and Ir(S-bt)$_2$(acac)-based devices.

is nearly three times of those for Ir(O-bt)$_2$(acac) and Ir(S-bt)$_2$(acac), the performance of Ir(SO$_2$-bt)$_2$(acac)-based device decreases significantly with high turn-on voltage of 6 V and low efficiencies of 3.5 cd A^{-1} and 1.6 lm W^{-1}. We propose the poor performance should be because complex Ir(SO$_2$-bt)$_2$(acac) is relatively harder to be evaporated, which may cause a low doping concentration in actual operation and finally results in adverse effect on the energy transfer from the excited host molecules to the ground-state dopants. The gradual efficiency roll-off with increasing current density was observed in the current efficiency-current density curves as shown in Figure 6. This efficiency roll-off is frequently observed for electrophoshporescent OLEDs and typically ascribed to triplet−triplet annihilation and electrical-field-induced quenching effect.[12,15]

In comparison with the vacuum deposited devices of above three complexes, the solution-processed device for complex Ir(PO-bt)$_2$(acac) exhibited further poor performance, with a relatively high turn-on voltage of 6 V, a maximum luminance L_{max} of 1057 cd m^{-2} at 13 V, and maximum efficiencies of 4.3 cd A^{-1} and 1.9 lm W^{-1}. The J−V−L characteristics and efficiency curves for the Ir(PO-bt)$_2$(acac) device is provided in Figure S3 in Supporting Information. The similar poor performance was also observed for other phosphoryl-based iridium complexes in literatures.[18] The poor device performance for the present Ir(PO-bt)$_2$(acac) was partially because the film quality of the solution-processed emitting layer is not comparable with those obtained by vacuum deposition.[11] It should be noted that all these preliminary data are subject to be further improved if device structures are optimized by such as introducing hole-transporting layer and exciton-blocking layers, or exploring most suitable doping concentration and film thickness.

On the basis of the good performance of the yellow-emitting iridium complexes in their single color devices, Ir(S-bt)$_2$(acac) was used in combination with a traditional blue phosphor to fabricate two-element white OLED (WOLED). The WOLED has a configuration of ITO/PEDOT:PSS (40 nm)/TAPC (10 nm)/CBP:Ir(S-bt)$_2$(acac) (3 wt %, 15 nm)/ CBP:Firpic (8 wt %, 15 nm/TmPyPB (30 nm)/LiF (1 nm)/Al (200 nm), in which TAPC (di-[4-(N,N-ditoly amino)-phenyl]cyclohexane) acts as the hole-injecting and electron-blocking layer because of its suitably high HOMO level of −5.5 eV and shallow LUMO level of −2.0 eV,[27,28] Firpic (iridium(III)bis(4,6-(difluorophenyl)pyridinato-N,C$^{2'}$)picolinate) as the blue-emitting phosphor, and TmPyPB (1,3,5-tri[(3-pyridyl)-phen-3-yl]benzene) as electron-transporting and hole-blocking layer because of its rather deep LUMO (−2.73 eV) and HOMO (−6.68 eV) levels.[29] In addition, both TAPC and TmPyPB function as exciton blocking layers that can confine the triplet excitons in emitting zone because of their higher triplet energies (E_T = 2.87 eV for TAPC, E_T = 2.78 eV for TmPyPB) than the yellow emitter Ir(S-bt)$_2$(acac) and the blue Firpic (E_T = 2.62 eV). As expected, the WOLED exhibited white emission over the whole detected voltage range. Figure 7 depicts the EL spectra at 14 V. Three intense emission peaks at 474, 502, and 562 nm, which are assigned to Firpic and Ir(S-bt)$_2$(acac), respectively. The CIE coordinates are (0.28, 0.44) at 14 V, which are close to those for the standard white light. The WOLED turned on at 4 V. As shown by the J−V−L characteristics and efficiency curves in Figure 8, the WOLED reached a maximum luminance of 19760 cd m^{-2} at 14 V, and a maximum luminance efficiency η_L of 32.4 cd A^{-1} (corresponding to η_p of 14.5 lm W^{-1}) at the current density of 0.337 mA cm^{-2}. Apparently, the high efficiencies of the white OLED should be at least ascribed to the good luminescent performance of the yellow-emitting Ir(S-bt)$_2$(acac).

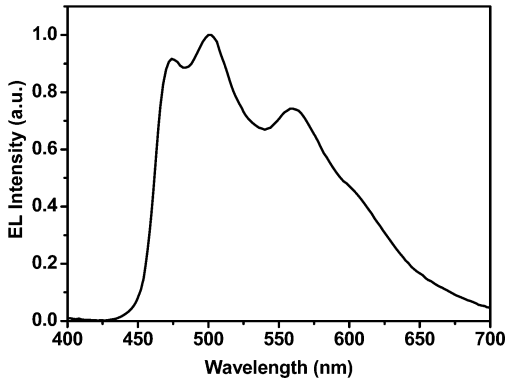

Figure 7. EL spectrum of the white OLED at 14 V.

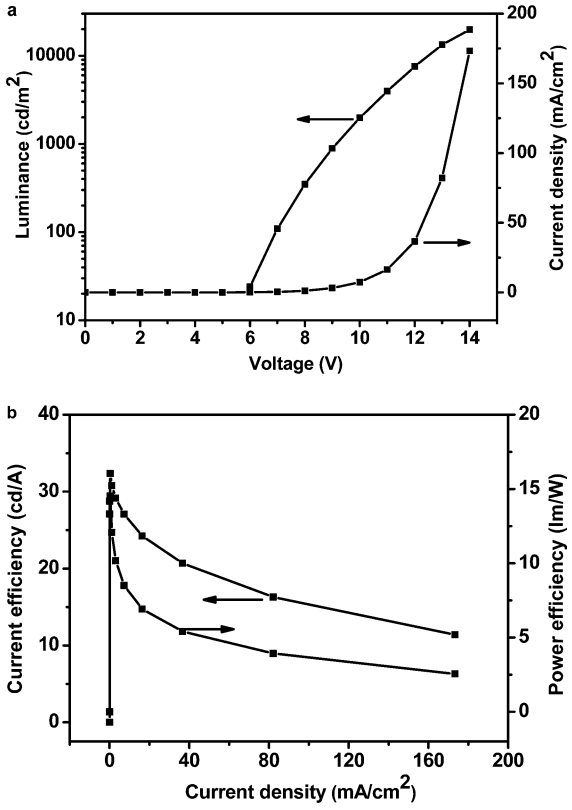

Figure 8. (a) J−V−L characteristics and (b) the efficiency curves for the white OLED with Firpic and Ir(S-bt)$_2$(acac) as doped emitters.

CONCLUSION

In conclusion, different from the traditional 2-phenylbenzothiazole ligand, we have developed a series of novel 2-arylbenzothiazole ligand frameworks with aryl being the aromatic groups other than phenyl, and prepared their heteroleptic iridium complexes. The room-temperature phosphorescence of these complexes is tunable from yellow to orange-red depending on the electronic properties of the aryl group. The strong electron-withdrawing aryls is favorable for relatively long emission wavelength. These complexes were used as doped emitters to fabricate OLEDs and good device performances were achieved. In particular, a maximum

efficiency of 58.4 cd A^{-1} (corresponding to 30.6 lm W^{-1} and 19%) with CIE coordinates of (0.45, 0.52) was achieved for Ir(O-bt)$_2$(acac) based yellow device, which are among the best data for the yellow OLEDs reported so far. The two-element white OLED was also fabricated with the yellow-emitting Ir(S-bt)$_2$(acac) and blue phosphor, reaching a high efficiency of 32.4 cd A^{-1}. The good performance indicates the potential application of these iridium complexes in large-scale OLED products.

■ ASSOCIATED CONTENT

Supporting Information

Synthesis of intermediates and ligands, and additional figures. This material is available free of charge via the Internet at http://pubs.acs.org.

■ AUTHOR INFORMATION

Corresponding Author

*E-mail: liudi@dlut.edu.cn.

Notes

The authors declare no competing financial interest.

■ ACKNOWLEDGMENTS

We thank the National Natural Science Foundation of China (21274016 and 21072026) and Fundamental Research Funds for the Central Universities (DUT13LK06) for financial support of this work.

■ REFERENCES

(1) Baldo, M. A.; O'Brien, D. F.; You, Y.; Shoustikov, A.; Sibley, S.; Thompson, M. E.; Forrest, S. R. *Nature* **1998**, *395*, 151−154.
(2) Wong, W. Y.; Ho, C. L. *Coord. Chem. Rev.* **2009**, *253*, 1709−1758.
(3) Jiang, X. Z.; Jen, A. K. Y.; Carlson, B.; Dalton, L. R. *Appl. Phys. Lett.* **2002**, *80*, 713−715.
(4) Kwong, R. C.; Sibley, S.; Dubovoy, T.; Baldo, M.; Forrest, S. R.; Thompson, M. E. *Chem. Mater.* **1999**, *11*, 3709−3713.
(5) Adachi, C.; Baldo, M. A.; Thompson, M. E.; Forrest, S. R. *J. Appl. Phys.* **2001**, *90*, 5048−5051.
(6) Baldo, M. A.; Lamansky, S.; Burrows, P. E.; Thompson, M. E.; Forrest, S. R. *Appl. Phys. Lett.* **1999**, *75*, 4−6.
(7) D'Andrade, B. W.; Thompson, M. E.; Forrest, S. R. *Adv. Mater.* **2002**, *14*, 147−151.
(8) Lamansky, S.; Djurovich, P.; Murphy, D.; Abdel-Razzap, F.; Lee, H. E.; Adachi, C.; Burrows, P. E.; Forrest, S. R.; Thompson, M. E. *J. Am. Chem. Soc.* **2001**, *123*, 4304−4312.
(9) Ho, C. L.; Chi, L. C.; Hung, W. Y.; Chen, W. J.; Lin, Y. C.; Wu, H.; Mondal, E.; Zhou, G. J.; Wong, K. T.; Wong, W. Y. *J. Mater. Chem.* **2012**, *22*, 215−224.
(10) Laskar, I. R.; Chen, T. M. *Chem. Mater.* **2004**, *16*, 111−117.
(11) Wang, R. J.; Liu, D.; Zhang, R.; Deng, L. J.; Li, J. Y. *J. Mater. Chem.* **2012**, *22*, 1411−1417.
(12) Wang, R. J.; Liu, D.; Ren, H. C.; Zhang, T.; Yin, H. M.; Liu, G. Y.; Li, J. Y. *Adv. Mater.* **2011**, *23*, 2823−2827.
(13) Chang, W. C.; Hu, A. T.; Duan, J. P.; Rayabarapu, D. K.; Cheng, C. H. *J. Organomet. Chem.* **2004**, *689*, 4882−4888.
(14) Zhang, B. H.; Tan, C. P.; Lam, C. S.; Yao, M.; Ho, C. L.; Liu, L. H.; Xie, Z. Y.; Wong, W. Y.; Ding, J. Q.; Wang, L. X. *Adv. Mater.* **2012**, *24*, 1873−1877.
(15) Wu, H. B.; Zhou, G.; Zou, J.; Ho, C. L.; Wong, W. Y.; Yang, W.; Peng, J. B.; Cao, Y. *Adv. Mater.* **2009**, *21*, 4181−4184.
(16) Jung, S.; Kang, Y.; Kim, H. S.; Kim, Y. H.; Lee, C. L.; Kim, J. J.; Lee, S. K.; Kwon, S. K. *Eur. J. Inorg. Chem.* **2004**, *17*, 3415−3423.
(17) Zhou, G. J.; Wang, Q.; Ho, C. L.; Wong, W. Y.; Ma, D. G.; Wang, L. X.; Lin, Z. Y. *Chem. Asian J.* **2008**, *3*, 1830−1841.
(18) Zhou, G. J.; Ho, C. L.; Wong, W. Y.; Wang, Q.; Ma, D. G.; Wang, L. X.; Lin, Z. Y.; Marder, T. B.; Beeby, A. *Adv. Funct. Mater.* **2008**, *18*, 499−511.
(19) King, K. A.; Spellane, P. J.; Watts, R. J. *J. Am. Chem. Soc.* **1985**, *107*, 1431−1432.
(20) Lamansky, S.; Djurovich, P.; Murphy, D.; Abdel-Razzaq, F.; Kwong, R.; Tsyba, I.; Bortz, M.; Mui, B.; Bau, R.; Thompson, M. E. *Inorg. Chem.* **2001**, *40*, 1704−1711.
(21) Li, J.; Li, Q.; Liu, D. *ACS Appl. Mater. Interfaces* **2011**, *3*, 2099−2107.
(22) Ren, H.; Li, J.; Wang, R.; Zhang, T.; Gao, Z.; Liu, D. *Polymer* **2011**, *52*, 3639−3646.
(23) Frisch, M. J.; Trucks, G. W.; Schlegel, H. B.; Scuseria, G. E.; Robb, M. A.; Cheeseman, J. R.; Montgomery, J. A., Jr.; Vreven, T.; Kudin, K. N.; Burant, J. C.; Millam, J. M.; Iyengar, S. S.; Tomasi, J.; Barone, V.; Mennucci, B.; Cossi, M.; Scalmani, G.; Rega, N.; Petersson, G. A.; Nakatsuji, H.; Hada, M.; Ehara, M.; Toyota, K.; Fukuda, R.; Hasegawa, J.; Ishida, M.; Nakajima, T.; Honda, Y.; Kitao, O.; Nakai, H.; Klene, M.; Li, X.; Knox, J. E.; Hratchian, H. P.; Cross, J. B.; Bakken, V.; Adamo, C.; Jaramillo, J.; Gomperts, R.; Stratmann, R. E.; Yazyev, O.; Austin, A. J.; Cammi, R.; Pomelli, C.; Ochterski, J. W.; Ayala, P. Y.; Morokuma, K.; Voth, G. A.; Salvador, P.; Dannenberg, J. J.; Zakrzewski, V. G.; Dapprich, S.; Daniels, A. D.; Strain, M. C.; Farkas, O.; Malick, D. K.; Rabuck, A. D.; Raghavachari, K.; Foresman, J. B.; Ortiz, J. V.; Cui, Q.; Baboul, A. G.; Clifford, S.; Cioslowski, J.; Stefanov, B. B.; Liu, G.; Liashenko, A.; Piskorz, P.; Komaromi, I.; Martin, R. L.; Fox, D. J.; Keith, T.; Al-Laham, M. A.; Peng, C. Y.; Nanayakkara, A.; Challacombe, M.; Gill, P. M. W.; Johnson, B.; Chen, W.; Wong, M. W.; Gonzalez, C.; Pople, J. A. *Gaussian 03*, revision C.02; Gaussian, Inc.: Wallingford, CT, 2004.
(24) Wang, R.; Liu, D.; Zhang, T.; Deng, L.; Wang, X.; Li, J. *Dalton Trans.* **2012**, *41*, 6833−6841.
(25) Yamamoto, H.; Wilkinson, J.; Long, J. P.; Bussman, K.; Christodoulides, J. A.; Kafafi, Z. H. *Nano Lett.* **2005**, *5*, 2485−2488.
(26) Hung, W. Y.; Chi, L. C.; Chen, W. J.; Chen, Y. M.; Chou, S. H.; Wong, K. T. *J. Mater. Chem.* **2010**, *20*, 10113−10119.
(27) Kulkarni, A.-P.; Kong, X.; Jenekhe, S.-A. *Adv. Funct. Mater.* **2006**, *16*, 1057−1066.
(28) Kalinowski, J.; Cocchi, M.; Virgili, D.; Fattori, V.; Williams, J. A. G. *Adv. Mater.* **2007**, *19*, 4000−4005.
(29) Bin, J.-K.; Cho, N.-S.; Hong, J.-I. *Adv. Mater.* **2012**, *24*, 2911−2915.